

# Persistent vs. arrested spreading of biofilms at solid-gas interfaces - the role of surface forces

Sarah Trinschek,<sup>1,2,3</sup> Karin John,<sup>2,3</sup> Sigolène Lecuyer,<sup>2,3</sup> and Uwe Thiele<sup>1,4,\*</sup>

<sup>1</sup>*Institut für Theoretische Physik, Westfälische Wilhelms-Universität Münster  
Wilhelm-Klemm-Strasse 9, 48149 Münster, Germany*

<sup>2</sup>*Univ. Grenoble Alpes, LIPHY, F-38000 Grenoble, France*

<sup>3</sup>*CNRS, LIPHY, F-38000 Grenoble, France*

<sup>4</sup>*Center of Nonlinear Science (CeNoS), Westfälische Wilhelms-Universität Münster  
Corrensstr. 2, 48149 Münster, Germany*

(Dated: June 29, 2018)

We introduce and analyze a model for osmotically spreading biofilm colonies at solid-air interfaces that includes wetting phenomena, i.e. surface forces. The model combines a hydrodynamic description for biologically passive liquid suspensions with bioactive processes. We show that wetting effects are responsible for a transition between persistent and arrested spreading and provide experimental evidence for the existence of this transition for *Bacillus subtilis* biofilms growing on agar substrates. In the case of arrested spreading, the biofilm is non-invasive albeit being biologically active. However, a small reduction in the surface tension of the biofilm is sufficient to induce spreading.

Biofilms are macro-colonies of bacteria enclosed in an extracellular matrix that form at diverse interfaces [1]. Cell proliferation and matrix production by the bacteria result in lateral spreading of the colony along the interface. Surprisingly, during the osmotic spreading of biofilms on moist solid (agar) substrates in contact with a gas phase, the spreading is not driven by the active motility of individual bacteria but by growth processes and the physico-chemical properties of the biofilm and the interfaces [2–4]. Within this mechanism, the biological production of polymeric matrix results in an osmotic flux of water from the agar into the biofilm that subsequently swells and spreads out. As the spreading involves the motion of a three-phase contact line between the viscous biofilm, the agar and the gas phase, wetting phenomena [5, 6] are likely to play an important role. This idea is supported by experiments, that indicate a strong dependence of biofilm spreading on their ability to produce biosurfactants [7–13].

To demonstrate the effect of surfactants, we perform osmotic biofilm spreading experiments using a *Bacillus subtilis* wild-type strain (WT) and a mutant strain with deficient production of surfactin ( $\Delta$ Srf) – a natural biosurfactant produced by WT *B. subtilis*. Typically, production is induced at high cell density by cell-to-cell communication (quorum sensing) [14, 15] and plays a key role in surface motility [16, 17].

Bacterial suspensions and agar substrates are prepared as described in note [18]. Agar plates with appropriate nutrient medium are inoculated with a small droplet of cell suspension, and biofilm growth and spreading is subsequently monitored. Figs. 1(a) and (b) show the colony of the WT and the mutant strain, respectively, after 3 days of incubation. The WT in (a) forms circular biofilms

with a diameter of about 2 cm whereas the mutant strain without *surfactin* in (b) is not able to spread. The external addition of *surfactin* shortly after agar inoculation has no effect on the spreading of the WT strain [Fig. 1(c)], but restores a WT morphology in the *surfactin*-deficient strain [Fig. 1(d)]. The WT phenotype can also be recovered by adding the non-physiological surfactants *Tween 20* [Figs. 1(e)-(f)] or *Span80* (not shown), which points at a physical role of *surfactin* in the spreading mechanism.

To model the influence of wetting phenomena on biofilm spreading we supplement a hydrodynamic description of a thin film of a biologically passive liquid suspension [19–21] by biomass growth processes. The recently introduced model [22] explicitly includes surface forces, i.e., wettability, via a Derjaguin (or disjoining) pressure and capillarity via the interface tensions. Sim-

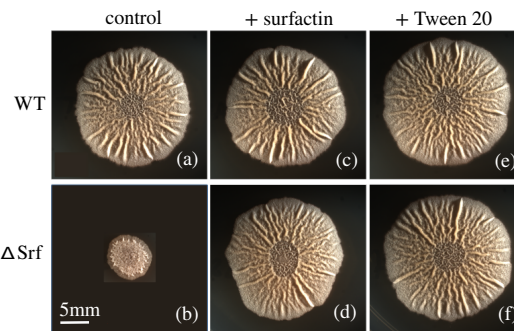


FIG. 1. Experimental observation of the influence of surfactants on the transition between persistent and arrested biofilm spreading. (a) The *B. subtilis* wild-type (WT) persistently spreads over the agar substrate, whereas (b) for the mutant strain with deficient surfactin production ( $\Delta$ Srf) spreading is arrested. An external addition of the surfactants (c,d) *surfactin* or (e,f) *Tween 20* enables the mutant strain to spread but does not affect the WT.

\* u.thiele@uni-muenster.de

ilar thin film models without wettability influences are used to study early stage biofilm growth and quorum sensing [23], osmotically driven spreading [2] and the effect of surfactant production on the spreading of a bacterial colony up a non-nutritive wall [11].

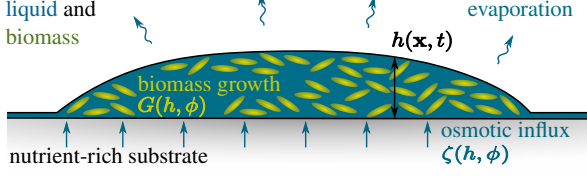


FIG. 2. Sketch of the osmotically driven spreading of a biofilm with the height profile  $h(\mathbf{x}, t)$ . Osmotic pressure gradients are generated as bacteria consume water and nutrients to produce biomass via bacterial proliferation and matrix secretion, which is described by the growth term  $G(h, \phi)$ . This causes an osmotic influx of nutrient-rich water  $\zeta(h, \phi)$  from the moist agar substrate into the biofilm.

Here, a biofilm of height  $h(x, y, t)$  is modelled as a mixture of solvent (nutrient-rich water) and of biomass (bacteria and extracellular polymeric matrix) with the height-averaged biomass concentration  $\phi(x, y, t)$  (see Fig. 2). The free energy functional, that determines all transport processes for the passive suspension is

$$F[h, \phi] = \int [f_w(h) + hf_m(\phi) + \frac{\gamma}{2}(\nabla h)^2] dA, \quad (1)$$

where  $\gamma$  is the biofilm-air surface tension and  $\nabla = (\partial_x, \partial_y)^T$  denotes the planar gradient operator. Furthermore,  $\gamma_{SG}$  and  $\gamma_{SL}$  are the solid-gas and solid-liquid interface energies. A common choice for the wetting energy is [6, 24]

$$f_w(h) = A\left(-\frac{1}{2h^2} + \frac{h_p^3}{5h^5}\right). \quad (2)$$

which combines destabilising long-range van-der-Waals and stabilising short-range interactions. Here,  $h_p$  denotes the height of a thin wetting layer and

$$A = \frac{10}{3}h_p^2(\gamma - \gamma_{SG} + \gamma_{SL}) \quad (3)$$

is the Hamaker constant, here expressed through the interface energies. For a partially wetting biofilm-substrate-air combination, minimizing Eq. (1) gives the coexistence of a wetting layer of height  $h_p$  with steady droplets of equilibrium contact angle  $\cos\theta_{eq} = 1 + f_w(h_p)/\gamma = (\gamma_{SG} - \gamma_{SL})/\gamma$ , equivalent to the Young-Dupré equation [5]. The film bulk contribution

$$f_m(\phi) = \frac{k_B T}{a^3} [\phi \ln(\phi) + (1 - \phi) \ln(1 - \phi)] \quad (4)$$

represents the entropic free energy of mixing of solute and solvent. We assume for simplicity, that biomass and

solvent are represented by the same microscopic length  $a$ .  $k_B T$  denotes the thermal energy.

The passive convective flux  $\mathbf{j}_{conv}$  and diffusive flux  $\mathbf{j}_{diff}$  are derived by applying a variational principle to the free energy (1) (for details see [21, 22]):

$$\mathbf{j}_{conv} = \frac{h^3}{3\eta} \nabla (\gamma \Delta h - \partial_h f_w) \quad (5)$$

$$\mathbf{j}_{diff} = -D_{diff} h \phi \nabla (\partial_\phi f_m). \quad (6)$$

The composition-dependent viscosity  $\eta$  of the biofilm [25–27] is given by  $\eta = (1 - \phi)\eta_0 + \phi\eta_b$ , where  $\eta_0$  and  $\eta_b$  denote the viscosity of solvent and biomass, respectively. The biomass diffusivity is  $D = \frac{a^2}{6\pi\eta}$  consistent with the diffusion constant  $D_{diff} = D \frac{k_B T}{a^3} = \frac{k_B T}{6\pi a \eta}$ .

The biomass multiplies by consuming nutrient-rich water following a bimolecular reaction  $g\phi(1 - \phi)$  with the growth rate constant  $g$ . To account for processes such as nutrient and oxygen depletion [3, 28] we introduce a limiting amount of biomass  $\phi_{eq} h^*$  by assuming a simple logistic growth law

$$G(h, \phi) = g\phi(1 - \phi)\left(1 - \frac{h\phi}{\phi_{eq} h^*}\right) \cdot f_{mod}(h, \phi). \quad (7)$$

$f_{mod}(h, \phi)$  [29] modifies the growth law locally for very small amounts of biomass. It ensures that at least one bacterial cell is needed for cell division and thus proliferation of biomass does not take place in the wetting layer.

Since the biomass cannot diffuse into the agar, biomass growth creates an osmotic imbalance between the biofilm and the agar. We assume, that the agar constitutes a large reservoir of nutrient rich water at a constant osmotic pressure  $\mu_{agar}$ , corresponding to an equilibrium water concentration  $(1 - \phi_{eq})$  in a flat biofilm. The osmotic pressure in the biofilm, defined as the negative of the variation of the free energy (1) with respect to the height  $h$  at a fixed number of osmotically active particles  $h\phi$ , is given by

$$\mu_s = -\frac{\delta F[h, \phi]}{\delta h} + \frac{\phi}{h} \frac{\delta F[h, \phi]}{\delta \phi} = -\partial_h f - g + \phi \partial_\phi g + \gamma \Delta h. \quad (8)$$

The osmotic flux of water between agar and biofilm depends linearly on the osmotic pressure difference  $\zeta(h, \phi) = Q_{osm} (\mu_s - \mu_{agar})$ , with  $Q_{osm}$  being a positive mobility constant.

Biomass growth and osmotic flux are incorporated into the model as two non-conserved terms  $G(h, \phi)$  and  $\zeta(h, \phi)$  which results in the following evolution equations for the effective layer thicknesses of liquid  $h$  and biomass  $h\phi$

$$\partial_t h = -\nabla \cdot \mathbf{j}_{conv} + \zeta(h, \phi) \quad (9)$$

$$\partial_t (h\phi) = -\nabla \cdot (\phi \mathbf{j}_{conv} + \mathbf{j}_{diff}) + hG(h, \phi). \quad (10)$$

Note that the conserved part of the dynamics can also be given in gradient dynamics form [21, 22, 30].

To facilitate the model analysis, we introduce vertical and horizontal length scales  $l = h_p$  and  $L = (\gamma/\kappa)^{1/2} l$ ,

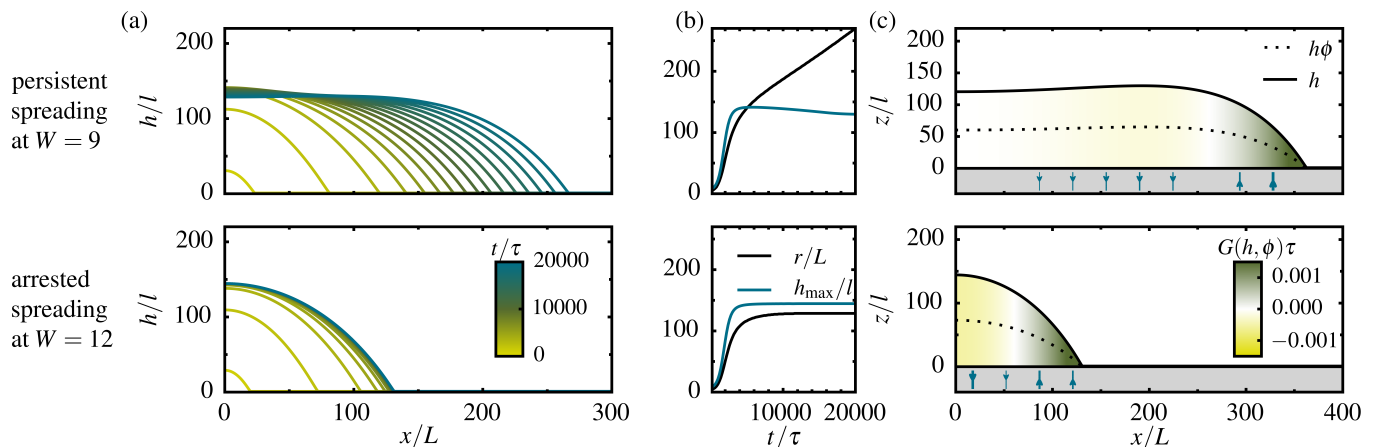


FIG. 3. Comparison of persistently spreading biofilms (top row, at  $W = 9$ ) and arrested spreading of biofilms (bottom row, at  $W = 12$ ). (a) Height profiles taken at equidistant times. (b) Time evolution of the biofilm extension  $r(t)$  (solid black) measured at the inflection point of the height profile, and of the maximal film height  $h_{\max}(t)$  (solid blue). (c) Bioactivity and osmotic influx for biofilms at a late time when all transients have decayed. The shading within the film indicates the bioactivity  $G(h, \phi)$ . The direction and strength of the effective osmotic flux  $\zeta(h, \phi)$  is represented by the direction and thickness of the blue arrows below the biofilm. Note that a time lapse of  $1000 \tau$  corresponds to  $\approx 5$  h. Remaining parameters are  $\tilde{g} = 0.01$  and  $\tilde{Q}_{\text{osm}} = 100$ .

respectively, with  $l \ll L$ , the time scale  $\tau = L^2 \eta_0 / \kappa l$  and the energy scale  $\kappa = k_B T l / a^3$ . This gives dimensionless growth rate  $\tilde{g} = g\tau$ , osmotic mobility  $\tilde{Q}_{\text{osm}} = Q_{\text{osm}} \tau \kappa / l^2$  and wettability parameter

$$W = \frac{A}{\kappa l^2} = \frac{A}{k_B T} \frac{a^3}{l^3} \quad (11)$$

that measures the relative strength of the wetting energy [31] as compared to the entropic free energy of mixing. Larger values of  $W$  correspond to a less wettable substrate and result in larger equilibrium contact angles.

Throughout the analysis we fix the maximal amount of biomass that can be sustained by the substrate to  $h^* \phi_{\text{eq}} = 60$ , the equilibrium water concentration to  $(1 - \phi_{\text{eq}}) = 0.5$  and the ratio of the viscosities of biomass and fluid to  $\frac{\eta_b}{\eta_0} = 20$ . The biofilm spreading behavior is studied depending on the growth rate  $\tilde{g}$ , the wettability parameter  $W$  and the osmotic mobility  $\tilde{Q}_{\text{osm}}$ . Comparing with the typical biofilm height of  $30 \mu\text{m}$  measured in [2] and using viscosity and surface tension of water ( $\eta_0 = 10^{-3} \text{ Pa s}$ ,  $\gamma = 70 \text{ mN/m}$ ) as well as the typical solvent/biomass length scale  $a = 100 \text{ nm}$ , this results in the vertical length scale  $l = h_p = 250 \text{ nm}$ , the lateral length scale  $L = 70 \mu\text{m}$  and the time scale  $\tau = 20 \text{ s}$ . With the above scales, a wettability parameter  $W = 10$  corresponds to an equilibrium contact angle of  $0.5^\circ$ , comparable to the dynamic contact angle measured in [2].

We analyze Eqs. (1-10) for a two-dimensional geometry (biofilm ridges instead of circular colonies) with no-flux boundaries employing numerical time simulations (finite element modular toolbox DUNE-PDELAB [32, 33] as previously used in [22, 30]) and continuation techniques [34] (software package *Auto-07p* [35]).

Our model (1-10) reproduces the non-equilibrium transition between persistently spreading biofilms and arrested spreading: On the one hand, at relatively high wettability (lower  $W$ , Fig. 3 (top, a) and (top, b)) the biofilm initially rapidly swells vertically and horizontally until a stationary film height is reached. Subsequently, it only spreads horizontally with a constant speed and shape of the biofilm edge. This qualitatively reproduces common experimentally observed behaviour [2, 4]. Fig. 3 (top, c) shows a snapshot of a spreading biofilm at a late time when all transients have decayed. Far from the advancing edges, the biofilm has reached the limiting amount of biomass and the biomass concentration corresponds to the equilibrium value  $\phi_{\text{eq}}$  so that all bioactive processes are in a dynamical equilibrium. At the edges, biomass growth takes place and causes an osmotic imbalance that results in a strong influx of water into the biofilm.

On the other hand, at lower wettability [larger  $W$ , Fig. 3 (bottom, a and b)], biofilm spreading is arrested. Again, the biofilm initially rapidly swells, however, in contrast to the case of higher wettability, it soon evolves towards a steady profile of fixed extension and contact angle. Note that the steady biofilm drops are still bioactive - Fig. 3 (bottom, c) shows that biomass is being produced at the biofilm edges where  $G > 0$  and is degraded at the centre where  $G < 0$  as there the biomass exceeds the limiting amount  $\phi_{\text{eq}} h^*$ . This is possible as hydrodynamic and diffusive fluxes within the biofilm and osmotic fluxes between agar and biofilm rearrange biomass and water such that their profiles are stationary.

The spreading behavior in dependence of wettability parameter  $W$  and the biomass growth rate  $\tilde{g}$  is summarized in the non-equilibrium phase diagram presented in Fig. 4. At constant  $\tilde{g}$ , corresponding, e.g., to a specific

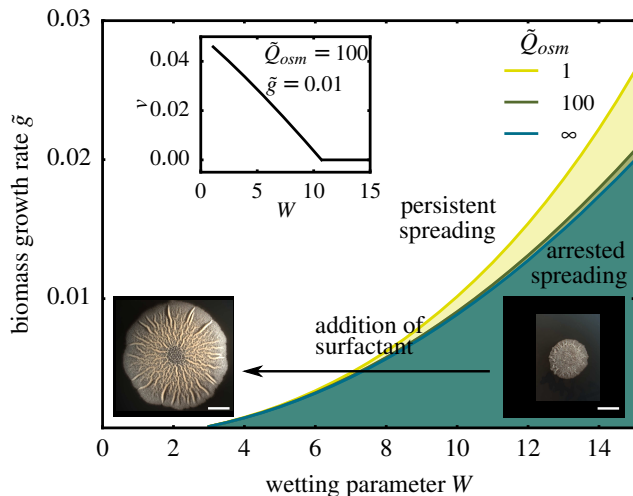


FIG. 4. Spreading behavior of the biofilm in the  $\tilde{g}$ - $W$  parameter plane for various values of the osmotic mobility  $\tilde{Q}_{osm}$  as indicated in the legend. In the shaded regions biofilm spreading is arrested, i.e., it reaches a steady profile while outside spreading is persistent. The inset gives the dependence of spreading speed  $v$  on wettability  $W$  for  $\tilde{g} = 0.01$  and  $\tilde{Q}_{osm} = 100$ . A speed of  $v = 0.01$  corresponds to an actual spreading speed of 0.1 mm/h, comparable to the experiment in [2]. (scale bar: 5 mm)

bacterial strain, spreading of the biofilm is arrested at low wettability (high value of  $W$ ). However, as adding a surfactant lowers the biofilm surface tension and, consequently, the parameter  $W \sim \gamma$  [cf. Eqs. (3) and (11)], it can trigger a transition from a non-invasive biofilm with arrested spreading to a persistently spreading biofilm – in agreement with the experimental results in Fig. 1 and Ref. [8].

This transition only slightly depends on the osmotic mobility  $\tilde{Q}_{osm}$  (see Fig. 4) and one may consider the limiting case of an instantaneous osmotic solvent transfer between agar and biofilm (i.e.,  $\tilde{Q}_{osm} \gg 1$ ). There,

the model reduces to a one-variable model for the evolution of the biofilm height [36], and still reproduces all relevant experimental features. Even for this infinitely fast osmosis, the parameter region of arrested spreading is only slightly smaller than for finite  $\tilde{Q}_{osm}$ . This indicates that thermodynamic forces (surface forces, entropic forces) rather than time scales of transport and bioactive processes are dominant in the determination of the transition between steady and invasive biofilms.

To summarize, we have presented a simple model for the osmotic spreading of biofilms that grow at solid-air interfaces. The model adds bioactive processes into a hydrodynamic approach and explicitly includes wetting effects. In consequence, it has allowed us to study the interplay between biological growth processes and passive surface forces. Our results have confirmed within a thermodynamically consistent framework that wetting crucially effects the spreading dynamics (invasiveness) of biofilms and has therefore provided a qualitative understanding of the experimentally observed transition between arrested and persistent spreading that occurs upon addition of external surfactants in a surfactin-deficient *B. subtilis* strain.

Our framework is limited to the biologically early stages of biofilm growth since it neglects all vertical gradients in the biofilm. However, it is well suited to model the dynamics of the spreading biofilm edge. In future extensions, one may incorporate the auto-production and dynamics of surfactants in the biofilm to consistently study the influence of Marangoni flows on the spreading dynamics [7, 9, 11]. As such flows are known to cause fingering instabilities in spreading surfactant-covered droplets [37] these mechanisms should be explored in connection to the branched structure described for some biofilm colonies.

## ACKNOWLEDGMENTS

We thank the lab of R. Losick at Harvard University for bacterial strains, the DAAD and Campus France (PHC PROCOPE grant 35488SJ) for financial support. LIPhy is part of LabEx Tec 21 (Invest. l’Avenir, grant ANR-11-LABX-0030).

- 
- [1] R. M. Donlan, *Emerg. Infect. Dis.* **8**, 881 (2002).
  - [2] A. Seminara, T. Angelini, J. Wilking, H. Vlamakis, S. Ebrahim, R. Kolter, D. Weitz, and M. Brenner, *Proc. Natl. Acad. Sci. USA* **109**, 1116 (2012).
  - [3] W. Zhang, A. Seminara, M. Suaris, M. P. Brenner, D. A. Weitz, and T. E. Angelini, *New J. Phys.* **16**, 015028 (2014).
  - [4] G. E. Dilanji, M. Teplitski, and S. J. Hagen, *Proc. R. Soc. B* **281** (2014).
  - [5] P.-G. De Gennes, *Rev. Mod. Phys.* **57**, 827 (1985).
  - [6] D. Bonn, J. Eggers, J. Indekeu, J. Meunier, and E. Rolley, *Rev. Mod. Phys.* **81**, 739 (2009).
  - [7] R. Daniels, S. Reynaert, H. Hoekstra, C. Verreth, J. Janssens, K. Braeken, M. Fauvart, S. Beullens, C. Heusdens, I. Lambrichts, *et al.*, *Proc. Natl. Acad. Sci. USA* **103**, 14965 (2006).
  - [8] V. Leclère, R. Marti, M. Béchet, P. Fickers, and P. Jacques, *Arch. Microbiol.* **186**, 475 (2006).
  - [9] M. Fauvart, P. Phillips, D. Bachaspatimayum, N. Verstraeten, J. Fransaer, J. Michiels, and J. Vermant, *Soft Matter* **8**, 70 (2012).
  - [10] W.-J. Ke, Y.-H. Hsueh, Y.-C. Cheng, C.-C. Wu, and S.-T. Liu, *Front Microbiol* **6**, 1017 (2015).

- [11] T. Angelini, M. Roper, R. Kolter, D. A. Weitz, and M. P. Brenner, *Proc. Natl. Acad. Sci. USA* **106**, 18109 (2009).
- [12] A. Be'er, R. S. Smith, H. Zhang, E.-L. Florin, S. M. Payne, and H. L. Swinney, *J. Bacteriol.* **191**, 5758 (2009).
- [13] R. De Dier, M. Fauvart, J. Michiels, and J. Vermant, in *The Physical Basis of Bacterial Quorum Communication* (Springer, 2015) pp. 189–204.
- [14] A. Oslizlo, P. Stefanic, I. Dogsa, and I. Mandic-Mulec, *Proc. Natl. Acad. Sci. USA* **111**, 1586 (2014).
- [15] J. van Gestel, H. Vlamakis, and R. Kolter, *PLoS Biol* **13**, e1002141 (2015).
- [16] P. D. Straight, J. M. Willey, and R. Kolter, *J. Bacteriol.* **188**, 4918 (2006).
- [17] D. B. Kearns and R. Losick, *Molecular microbiology* **49**, 581 (2003).
- [18] *Bacillus subtilis* strains NCBI3610 and its surfactin mutant  $\Delta SrfAA :: mls$  were streaked from  $-80^{\circ}\text{C}$  stocks on LB agar plates (1.5% bacto-agar) and grown at  $37^{\circ}\text{C}$  overnight. In the morning, a few colonies were scraped from the plate and resuspended in LB medium to an optical density of 1 ( $\text{OD}_{600}=1$ ). For colony growth assays,  $2\ \mu\text{L}$  of this solution were spotted at the center of an agar plate (1.5% agar) prepared with the minimal biofilm-inducing medium MSgg (5 mM potassium phosphate, 100 mM MOPS (pH 7), 2 mM  $\text{MgCl}_2$ , 50  $\mu\text{M}$   $\text{MnCl}_2$ , 50  $\mu\text{M}$   $\text{FeCl}_3$ , 700  $\mu\text{M}$   $\text{CaCl}_2$ , 1  $\mu\text{M}$   $\text{ZnCl}_2$ , 2  $\mu\text{M}$  thiamine, 0.5% glycerol, 0.5% sodium glutamate, 50  $\mu\text{g}\cdot\text{ml}^{-1}$  threonine, 50  $\mu\text{g}\cdot\text{ml}^{-1}$  tryptophan, and 50  $\mu\text{g}\cdot\text{ml}^{-1}$  phenylalanine). Plates were then incubated at  $30^{\circ}\text{C}$  for 3 days, in a high humidity chamber. To test the effect of an external addition of surfactants,  $5\ \mu\text{l}$  of a 5 mM solution of purified surfactin, Tween 20 or Span 80 (all from Sigma-Aldrich) were spotted on top of the bacterial inoculate at  $t_0$ . Colonies were imaged at low magnification using a stereoscope (Zeiss Discovery.v8) equipped with a video camera and a computer interface.
- [19] U. Thiele, D. V. Todorova, and H. Lopez, *Phys. Rev. Lett.* **111**, 117801 (2013).
- [20] U. Thiele, *EPJ ST* **197**, 213 (2011).
- [21] X. Xu, U. Thiele, and T. Qian, *J. Phys.: Condens. Matter* **27**, 085005 (2015).
- [22] S. Trinschek, K. John, and U. Thiele, *AIMS Materials Science* **3**, 1138 (2016).
- [23] J. Ward and J. King, *J. Eng. Math.* **73**, 71 (2012).
- [24] U. Thiele, in *Thin Films of Soft Matter*, edited by S. Kalliadasis and U. Thiele (Springer, Wien, 2007) pp. 25–93.
- [25] L. Hall-Stoodley, J. W. Costerton, and P. Stoodley, *Nat. Rev. Microbiol.* **2**, 95 (2004).
- [26] I. Sutherland, *Microbiology* **147**, 3 (2001), cited By 662.
- [27] P. C. Lau, J. R. Dutcher, T. J. Beveridge, and J. S. Lam, *Biophys. J.* **96**, 2935 (2009).
- [28] L. E. Dietrich, C. Okegbe, A. Price-Whelan, H. Sakhtah, R. C. Hunter, and D. K. Newman, *J. Bacteriol.* **195**, 1371 (2013).
- [29] The explicit form of  $f_{\text{mod}}(h, \phi)$  is chosen as
- $$f_{\text{mod}}(h, \phi) = \left(1 - \frac{\psi_{2,u}}{\phi_2 h}\right) (1 - \exp(\phi_{\text{eq}} h_p - \phi h)) \quad (12)$$
- but other choices for  $f_{\text{mod}}(h, \phi)$  with the same fix point structure do not change the results qualitatively.
- [30] M. Wilczek, W. B. Tewes, S. V. Gurevich, M. H. Köpf, L. Chi, and U. Thiele, *Math. Model. Nat. Phenom.*, 44 (2015).
- [31] L. M. Pismen and U. Thiele, *Phys. Fluids* **18**, 042104 (2006).
- [32] P. Bastian, M. Blatt, A. Dedner, C. Engwer, R. Klöforn, R. Kornhuber, M. Ohlberger, and O. Sander, *Computing* **82**, 103 (2008).
- [33] P. Bastian, M. Blatt, A. Dedner, C. Engwer, R. Klöforn, R. Kornhuber, M. Ohlberger, and O. Sander, *Computing* **82**, 121 (2008).
- [34] H. A. Dijkstra, F. W. Wubs, A. K. Cliffe, E. Doedel, I. Dragomirescu, B. Eckhardt, A. Gelfgat, A. L. Hazel, V. Lucarini, A. G. Salinger, *et al.*, *Commun. Comput. Phys.* **15**, 1 (2014).
- [35] E. Doedel and B. Oldeman, *AUTO07p: Continuation and bifurcation software for ordinary differential equations*, Concordia Univerity (2009).
- [36] If the influx of water is fast as compared to biomass growth, but not as fast as the hydrodynamic fluxes, one can reduce the model to an effective description of the biofilm height as the large biofilm droplets are always in 'osmotic equilibrium'  $\mu_s = \mu_{\text{agar}}$  with the substrate on the time scale of the biomass growth with
- $$\zeta(h, \phi) = \frac{1}{1 - \phi_{\text{eq}}} G(h, \phi).$$
- The evolution equation for the total height reduces to
- $$\partial_t h = \nabla \cdot \left[ \frac{h^3}{3\hat{\eta}} \nabla (\partial_h f - \Delta h) \right] + \frac{1}{1 - \phi_{\text{eq}}} G(h, 1 - \phi_{\text{eq}})$$
- with a constant viscosity  $\hat{\eta} = \phi_{\text{eq}} + k_{\eta}(1 - \phi_{\text{eq}})$ .
- [37] O. K. Matar and S. M. Troian, *Phys. of Fluids* **11**, 3232 (1999).